La mer 61 : 1–11, 2023, https://doi.org/10.32211/lamer.61.1-2_1
Société franco-japonaise d'Océanographie, Tokyo

Occurrence patterns and feeding habits of *Tridentiger obscurus* in Furuhama Park, Ota City, Tokyo, central Japan

Keita MARUYAMA[1, 2)]*, Chihiro KANEKO[1)] and Hiroshi KOHNO[1, 3)]

Abstract: The occurrence patterns and feeding habits of the gobiid *Tridentiger obscurus* were investigated to clarify the habitat use in an urban seaside park constructed in the inner Tokyo Bay. Surveys were conducted using small seine nets and net cages on an artificial sandy beach, a tidal flat, and a seawall in Furuhama Park, Ota City, Tokyo. In total, 119 individuals (6.3–46.6 mm body length [BL], mode of BL was 5.0–9.9 mm) were collected from the sandy beach; 89 (6.2–42.6 mm, 10.0–14.9 mm) from the tidal flat; and 1,092 (8.0–73.7 mm, 40.0–44.9 mm) from the seawall. On the sandy beach and tidal flat, the goby fed mainly on zooplankton by 11.0 mm BL, and thereafter on small benthic and epibenthic crustaceans in addition to the zooplankton as they grew. On the seawall, *T. obscurus* fed on small benthic and epibenthic crustaceans with no ontogenetic diet shift. These results revealed that *T. obscurus* would grow by taking different prey resources among multiple environments in the urban seaside park during their early life history, implying the need for comprehensive conservation of the various environments to protect the fish species.

Keywords : *Gobiidae, Ontogenetic dietary shift, Artificial environment, Tokyo Bay*

1. Introduction

Tokyo Bay is a closed bay located near the center of Japan and opens to the Pacific Ocean. The bay is surrounded by Tokyo, Chiba, and Kanagawa prefectures, and one of the most developed sea areas in Japan. The inner Tokyo Bay is defined as the bay area of north side of the line connecting Futtsu in Chiba Prefecture and Kannonzaki in Kanagawa Prefecture (KOHNO *et al.*, 2011).

The inner Tokyo Bay with vast tidal flats had been one of the most productive fishing areas in Japan by the 1960s (SHIMIZU, 1990). However, as the economy began to develop, the pollution load to the inner bay began to increase in the 1950s, and water quality problem became more serious. Furthermore, the reclamation of many tidal flats and shallow areas from the 1960s led to a decrease in fish and shellfish catches, and the area became known as the "Sea of Death" (SHIMIZU,

1) Laboratory of Ichthyology, Tokyo University of Marine Science and Technology, 4–5–7 Konan, Minato-ku, Tokyo 108–8477, Japan
2) Graduate School of Science and Technology for Innovation, Yamaguchi University, 2–16–1 Tokiwadai, Ube, Yamaguchi, 755–8611, Japan
2) Nagao Natural Environment Foundation, 4–20–9 Midori, Sumida-ku, Tokyo 130–0021, Japan
* Corresponding author:
E-mail: bokuwamoku@gmail.com

1999). Thus, the area of tidal flats, which was estimated to be 136 km^2 before the 1940s, decreased to 10 km^2 in 1973 (OGURA, 1993). Since the 1970s, multiple administrative agencies along the coast of the Tokyo Bay have created artificial tidal flats to revitalize the area so that citizens can enjoy ecosystem services again (YAMANE *et al*., 2004; KOHNO *et al*., 2008). As a result, the area of tidal flats increased to 16.4 km^2 in 1997 (MINISTRY OF THE ENVIRONMENT OF JAPAN, 1997), but the vast mudflats and shallow areas in the past have been lost and much of the coastline have been replaced by seawalls and artificially placed rocky areas (SHIMIZU, 1999; ONODERA *et al*., 2020).

Owing to the loss of these tidal flats and shallow areas, which served as important habitats for fish, there are only few natural tidal flats left to serve this function (KANOU *et al*., 2000; HERMOSILLA *et al*., 2012). Under this situation, comprehensive surveys have been conducted on artificial tidal flats in Tokyo Bay; for example, Kasai Marine Park (KUWABARA *et al*., 2003; YAMANE *et al*., 2004) and Furuhama Park in Tokyo (MURAI *et al*., 2016; MARUYAMA *et al*., 2021); Shinhama-ko Lagoon in Chiba Prefecture (KOHNO *et al*., 2008); and Hakkei-jima Park in Kanagawa Prefecture (YAMANE *et al*., 2004). These surveys revealed that artificial tidal flats would function as nursery grounds for various fish species.

Moreover, similar surveys have been performed on vertical seawalls and rocky shorelines, which make up the majority of the inner Tokyo Bay; for example, the ichthyofauna of vertical seawalls (SAKAI *et al*., 2007; ONODERA *et al*., 2020) and the occurrence patterns of gobies in rocky areas (MURASE *et al*., 2007). However, these surveys have mainly focused on ichthyofauna, and there have been few studies on the detailed occurrence patterns and feeding habits of each fish species. Currently, while planning the restoration of lost tidal flats and shallow areas, the need to clarify environment preferences and food habits in each developmental stage in each fish species has been pointed out (MURAI *et al*., 2016; MARUYAMA *et al*., 2021).

The tripletooth goby *Tridentiger obscurus* is typical estuarine fish, widely distributed in brackish waters in Japan (KISHI, 2001). In this study, we investigated ecological information such as the occurrence patterns and feeding habits of the goby in an urban seaside park of the inner Tokyo Bay in order to clarify the habitat use of resident fish in several artificial environments in the bay area.

2. Materials and Methods

The survey site is Furuhama Park, located in Ota City, Tokyo, on the western shore of the inner Tokyo Bay (Fig. 1). Furuhama Park was opened in 2007 as a park with 1.2 ha of sandy beach (median particle size = 0.2 mm mountain sand from Kimitsu, Chiba Prefecture, hereinafter referred to as "sandy beach"); 1.0 ha of muddy tidal flat (a native tidal flat relocated 200 m offshore and covered with porous gravel and rocks, hereinafter referred to as "tidal flat"); and a 4.6 ha shallow area with water depth of 1.5 m between the sandy beach and tidal flat (TAKEYAMA *et al*., 2018). Submerged dikes, approximately 4.0 m high from the seafloor, are located at the northern and southern ends of the shallow area that borders the surrounding canal. Submerged dikes control the discharge of sediment from shallow areas and the inflow of hypoxic oxygen water spreading to the bottom layer of the surrounding canals (OKAMURA *et al*., 2004). Environmental and ichthyofaunal surveys have been conducted on this park since before its construction (e.g., OTA CITY, 2019; TAKEYAMA *et al*., 2018) and there are many previously reported studies

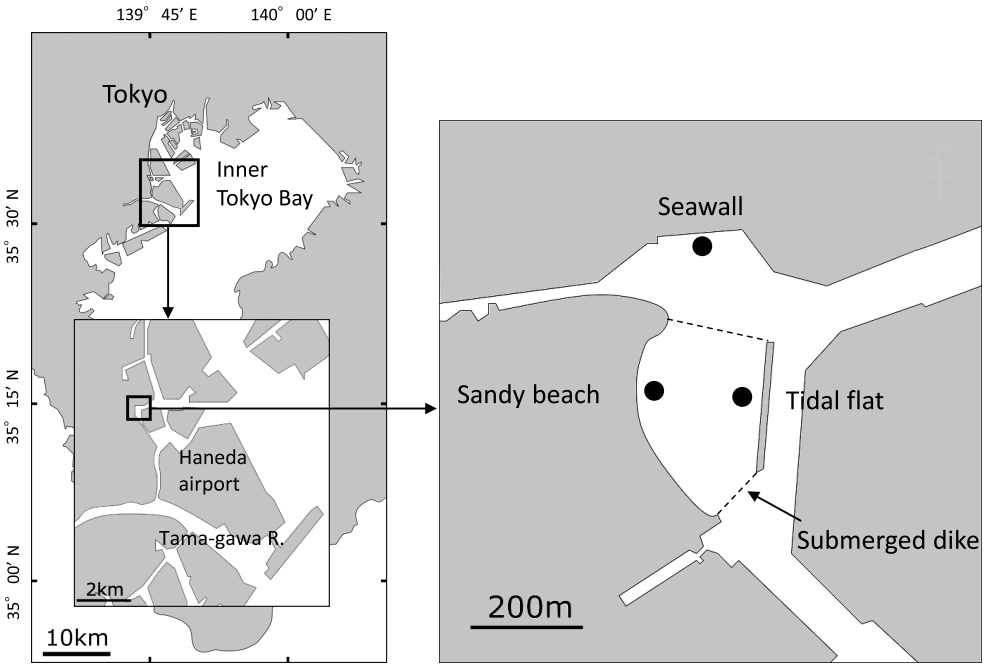

Fig. 1 Map showing the sampling sites in Furuhama Park located in inner Tokyo Bay. Fish were caught with a small seine net in the sandy beach and tidal flat and with net cages in the seawall.

on them, which are unusual for an urban waterfront park.

The study site and surrounding waters are brackish, and the annual mean salinity is 17.4 on the beach and 18.0 on the tidal flat (MARUYAMA *et al*., 2021). The average dissolved oxygen (herelnafter DO) is more than 7.0 mg/L through years on sandy beach and tidal flat and have never been below 3.0 mg/L; however, the bottom layer of the surrounding canal area becomes hypoxic, causing the DO level to be below 3.0 mg/L during summer (TAKEYAMA *et al*., 2018; ONODERA *et al*., 2020). There are no *Sargassum* or *Zostera* beds, and many vertical seawalls made of concrete and rocky areas, which are characteristic of urban canal areas, exist in the surrounding area.

Fish samples were collected at three stations: sandy beach, tidal flat, and seawall (Fig. 1). On the sandy beach and the tidal flat, surveys were conducted once a month from May 2014 to April 2019 using seine nets at low tide during the daytime around the spring tide. However, the tidal flat was not surveyed in September and October 2014, January and June 2015, and April 2019. In 2016 and 2017, the surveys could not be conducted in August; therefore, they were conducted twice in September. The number of tows of small seine nets was two (three in May and June 2014). A small seine net (sleeve net: 4.5 m long, 1.0 m high, mesh size 2.0 mm; body to bag net: 2.0 m wide, 1.0 m high, 5.5 m long, 0.8 mm mesh) (KANOU *et al*., 2002) was used for the survey and towed 25 m along the shoreline at a depth of 1.0 m or less. The net was towed such that the width of the net opening was 4.0 m. In this case, 100 m^2 of fish was collected at a time.

Sampling surveys were conducted on the sea-

wall from April 2016 to March 2019 using a fishing gear called a net cage. Three types of net cages were prepared by placing different internal materials (nylon net, bamboo shoot, and oyster shell) in a wire mesh cage (0.4 m in length and width, 0.5 m in height, 40 mm mesh size), as described by TAKEYAMA *et al.* (2017). The net cages for each internal material were set with ropes at two points, one at the water surface and the other at the seafloor, and sampling was conducted once a month at low tide during the daytime around the spring tide. The water surface cages were anchored to a floating pier that moved with the tides, so that they were always positioned at the water surface. The net cages that had been collected were sunk in the same position and collected again the following month in the same manner. In collecting the fish, we hauled the fish with the rope, retrieved the net cage, and collected the fish in the cages. To prevent fish from escaping from the net cage, the bottom and surrounding areas of the net cage were covered with a scoop net (opening size 1.1 m, mesh size 1.0 × 1.0 mm). The differences in fish occurrence patterns by materials and depth are discussed in detail in ONODERA *et al.* (2020) and TAKEYAMA *et al.* (2017), so this paper treats all *Tridentiger obscurus* collected in the seawall together. At the study site, it has been shown that the hypoxic water occurs in the bottom layer during the summer months, making it difficult for fish to inhabit.

The samples were fixed in the field using 10% brackish water formalin and brought to the laboratory. *Tridentiger obscurus* specimens were sorted and identified from the samples in the laboratory, counted, measured for body length [BL], and their developmental stages were determined. The developmental stages of the samples were classified into three classes (larvae: when the number of fin rays had not completed; juvenile: when the number of fin rays had completed but the fish was still immature; adult: when the fish was sexually mature) based on KANOU *et al.* (2000). In this study, samples with 9.9 mm BL or less were classified as larva, 10.0–29.9 mm BL as juvenile, and 30.0 mm BL or more as adults.

A total of 218 individuals were used as samples for feeding habit analyses: 22 individuals (7.0–15.5 mm BL) collected on the sandy beach, 39 individuals (7.0–30.3 mm) on the tidal flat, and 157 individuals (11.2–68.3 mm) on the seawall. Volumetric analysis (HYSLOP, 1980) was used to examine their gut contents, and the mean volume percentage (%V) was calculated according to HORINOUCHI and SANO (2000) and KANOU *et al.* (2004). The food items in the gut contents of each individual were identified as the lowest possible taxon. The anterior half of the gut was examined for larvae with a straight gut, and the gut contents up to the first bending were examined for individuals with a bent gut. The volume of gut contents was determined as follows: the gut contents of each individual were observed under a binocular microscope to assess the diet and the volume of each food item was determined on a glass slide with a 1.0 × 1.0 mm grid pattern, aligned with the thickness. In each individual, the volumes of all food items were added and the total volume of the gut contents was calculated. The percentage of the volume of each food item was calculated from the total calculated volume. Specimens with empty guts were excluded from the analyses. To determine whether the feeding habits changed with growth, the Mann-Whitney *U*-test was used to test whether there was a difference in the %V of major food items among several length ranges.

3. Results

3.1 Occurrence patterns

The number of *Tridentiger obscurus* collected

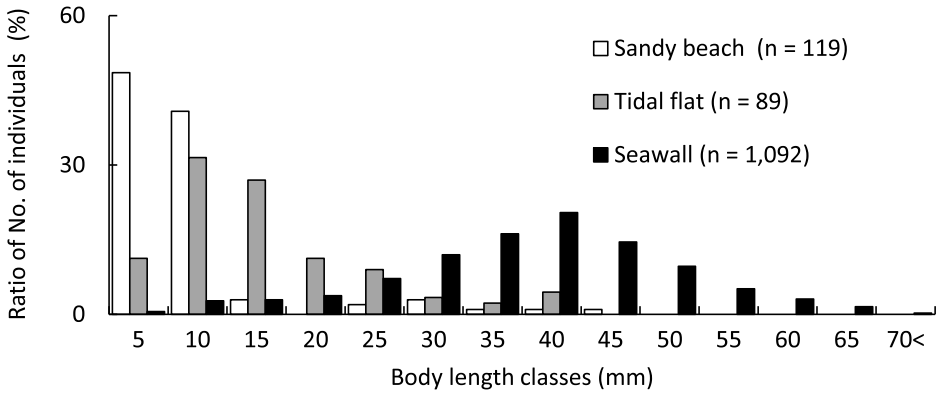

Fig. 2 Body length classes of *Tridentiger obscurus* collected from Furuhama Park during the study period from 2014 to 2019, shown by each collecting site.

was 119 individuals (6.3–46.6 mm in body length, BL) on the sandy beach, 89 individuals (6.2–42.6 mm BL) on the tidal flat, and 1,092 individuals (8.0–73.7 mm BL) on the vertical seawall (Fig. 2). The mode of body lengths classes from 5.0 to 9.9 mm for the sandy beach, 10.0 to 14.9 mm for the tidal flat, and 40.0 to 44.9 mm for the seawall. In addition, 40.0–44.9 mm were collected in abundance on three materials of the net cages. The goby occurred from March to October on the sandy beach, January to November on the tidal flat, and throughout the year on the seawall. The number of individuals collected on the sandy beach was high from July to October and low from January to June (Fig. 3). On the tidal flat, relatively large numbers of individuals were collected from April to June and few individuals throughout the year. On the vertical seawall, a certain number of individuals were collected throughout the year, but the number was particularly high from July to September.

In terms of developmental stages, larvae and juveniles appeared in the same proportion on the sandy beach from July to September, but more larvae were observed in October (Fig. 3). On the tidal flat, most fish were juveniles from January to June; however, adults were observed in addition to juveniles from July to September, and larvae and juveniles appeared in the same proportions in October and November. On the vertical seawall, adults were abundant throughout the year and almost no larvae were observed. Juveniles were also observed throughout the year and were abundant from July to September.

3.2 Feeding habits

Tridentiger obscurus on the sandy beach and tidal flat fed mainly on zooplankton, such as calanoid copepods (65.6% and 88.4%, respectively), followed by small benthic and epibenthic crustaceans, such as amphipods and mysids (Fig. 4). However, the %Vs of zooplankton were significantly different between the two stations after they attained 11.0 mm BL ($p<0.05$), with a mean percentage of 23.8% on the sandy beach and 48.4% on the tidal flat, indicating that *T. obscurus* larger than 11.0 mm BL shifted to and fed primarily on small benthic and epibenthic crustaceans. In contrast, *T. obscurus* on the seawall did not show a diet shift with growth; they mainly fed on small benthic and epibenthic crustaceans, such as amphipods, and polychaetes (Fig. 4). No individuals of *T. obscurus* feeding on fish includ-

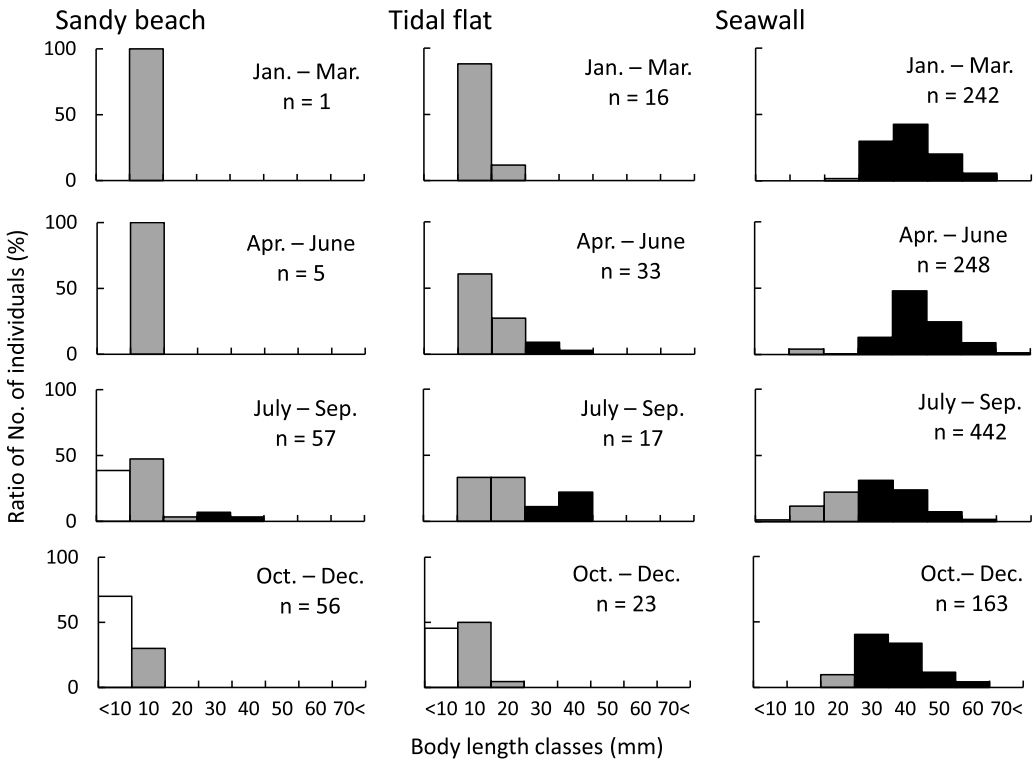

Fig. 3 Body length classes of *Tridentiger obscurus* collected at each habitat for every three months from May 2014 to April 2019. Open bars indicate the larva, gray bars indicate the juvenile, and solid bars indicate the adult.

ing this species were observed.

The percentage of empty gut was 0% on the sandy beach, 2.6% (1 individual) on the tidal flat, and 4.0% (6 individuals) on the vertical seawall.

4. Discussion

4.1 Habitat shifts with growth

The number of *Tridentiger obscurus* larvae smaller than 9.9 mm BL collected in this study was 59 out of 119 individuals (49.6%) at the sandy beach and 10 out of 89 (11.2%) at the tidal flat. NAKAMURA (1942) reported that *T. obscurus* up to 9.35 mm BL is considered to be pelagic larvae. Many gobiid species in Tokyo Bay have a pelagic life during the larval stage, and such larvae have been shown to have poor swimming abilities (ANGMALISANG *et al.*, 2020; NAKAIMUKI *et al.*, 2022). Therefore, the sandy beach and tidal flat in Furuhama Park, which are less affected by waves, may provide pelagic life area for the *T. obscurus* larvae.

Although *Tridentiger obscurus* rarely appeared on the sandy beach after reaching 15.0 mm BL (11 individuals occupying 9.2%), they appeared in some numbers on the tidal flat (51 individuals occupying 57.3%) and were abundant on the seawall (1,059 individuals occupying 97.0%). In Furuhama Park, hand net sampling was conducted twice a year (in June, September, or October) as a post-construction environmental survey in Ota City. Among them, results from a rocky area approximately 50 m west of

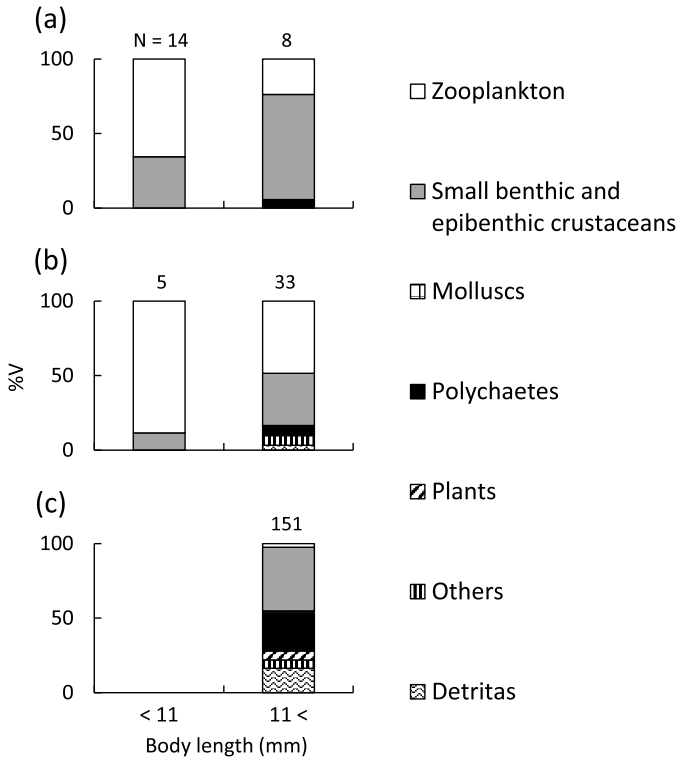

Fig. 4 Percentage volume (%V) of food items in the guts of *Tridentiger obscurus* in each habitat (a: sandy beach; b: tidal flat; c: seawall) from May 2014 to April 2019. Numerical characters on top of each column indicate the number of fish with food examined.

the seawall in the present study site showed that *T. obscurus* of 7–90 mm BL were collected, and the mode was 45.1–50.0 mm BL (OTA CITY, 2015–2019). *T. obscurus* generally congregate in estuarine areas where there are gravels, boulders, and artificial dumping sites (KISHI, 2001; KOHNO *et al.*, 2011). Recently, *T. obscurus* was reported to be abundant on seawalls in urban canal areas (TAKEYAMA *et al.*, 2017; ONODERA *et al.*, 2020). Therefore, *T. obscurus* select habitats according to their developmental stages, such that they initially grow on sandy beach and tidal flat up to 15.0 mm BL and then change habitat to seawall and/or rocky areas where they grow to 15.0 mm BL and larger.

From the juvenile stage, *Tridentiger obscurus* has a habit of getting under cover and prefers areas with boulders and artificial dumping rather than open areas (Kohno et al, 2011). Some individuals larger than 15.0 mm BL were observed on the tidal flat, probably because of the presence of boulders of various sizes (10–50 cm in diameter) scattered on the tidal flat. Although these boulder areas have been shown to be feeding areas for birds, such as *Arenaria interpres* and *Numenius phaeopus* (OTA CITY, 2018), they may provide important microhabitats for other organisms such as fish.

4.2 Ontogenetic dietary shift

At both the sandy beach and tidal flat, *Tridentiger obscurus* fed mainly on zooplankton such as calanoid copepods when they were up to 11.0 mm BL, but when they grew to a size larger than 11.0 mm BL as juveniles, the proportion of zooplankton in their gut contents decreased and they started feeding on small benthic or epibenthic crustaceans such as amphipods and mysids. These results indicate that these two stations function as ontogenetic dietary shift areas.

The timing of these diet shift has been studied in other gobiids; for example, *Acanthogobius flavimanus*, which are dominant species on tidal flats in the inner Tokyo Bay, change their main food items from zooplankton such as calanoid and cyclopoid copepods and cladocerans to small benthic and epibenthic crustaceans such as harpacticoid copepods and gammaridean amphipods and polychaetes when juvenile fish settle on the bottom (KANOU *et al*., 2004). Although *Tridentiger obscurus* entered the juvenile stage at 10.0 mm BL in this study, HWANG *et al.* (2006) mentioned that the size format which they change from larval to juvenile was 11.6–14.3 mm BL. NAKAMURA (1942) indicated that *T. obscurus* shifted to a benthic lifestyle at 9.35 mm BL. From these results, it is clear that *T. obscurus* change their main food items as they settle on the bottom during transformation period from larvae to juveniles.

The present study revealed that *Tridentiger obscurus* on the seawall at Furuhama Park fed mainly on small benthic or epibenthic crustaceans such as amphipods and polychaetes. Therefore, food habits of *T. obscurus* after the juvenile were common; however, they expand their habitat from sandy beach and tidal flat to seawall and rocky areas after changing their main food items from zooplankton to small benthic and epibenthic crustaceans in the former nurseries. Although it has been reported that *T. obscurus* in the inner Tokyo Bay fed heavily on algae (KANOU *et al*., 2004; MURASE *et al*., 2013), the %V of algae in this study was low (6.1 %). In Lake Hinuma, Ibaraki Prefecture, the main prey of 31–52 mm BL *T. obscurus* was mysids (KANEKO *et al*., 2016). During sampling in the present study, many amphipods were observed to be attached to net cages and on boulders in the tidal flat. In addition, it has been reported that many amphipods inhabit seawalls and boulder areas, which are the research locations in this study (OGAWA, 2011), and it is possible that *T. obscurus* used to prefer to feed on amphipods in Furuhama Park. This supports the idea that the feeding habit of *T. obscurus* varies according to environmental conditions (MURASE *et al*., 2013); thus, the species is classified as a miscellaneous/opportunist, rather than an omnivore.

4.3 Spawning ground and seasons

The smallest specimen of *Tridentiger obscurus* captured in this study was a 6.2 mm BL and was collected on the tidal flat, and hatching larvae have been reported to be 3.1 mm BL (NAKAMURA, 1942). HWANG *et al.* (2018), who bred *T. obscurus* in aquaria and observed the larvae and juveniles, reported that *T. obscurus* grew to 2.83–4.07 mm in total length [TL] at 8 days after hatching, 3.63–4.93 mm TL at 17 days, and 7.18–8.73 mm TL at 28 days. NAKAMURA (1942) reported that the TL of *T. obscurus* larvae is 105.1 to 118.9% of BL. Thus, the smallest specimen collected in this study was estimated to be 6.5–7.4 mm TL, indicating that the specimen was between 17 and 28 days post-hatching.

The smallest mature BL of *Tridentiger obscurus* is 27 mm for males and 30 mm for females (NAKAMURA, 1942). Many larger adult individuals were observed in this study, particularly on the seawall station. In addition, many adults

have been found on the rocky areas in Furuhama Park (OTA CITY, 2015–2019). The spawning season of *T. obscurus* in Tokyo Bay is from May to September (KISHI, 2001), and larvae were observed from July to November on the sandy beach and tidal flat. In May 2017, during the period of this study, *T. obscurus* were observed to spawn and protect their eggs on the inner surface of dead oyster shell (*Crassostrea gigas*) attached to the seawall. Based on these reports, the area around Furuhama Park, including the seawall, may be a spawning ground for *T. obscurus,* and the spawning season is estimated to be from May to October. These findings indicate that artificial environments may not only provide habitats for each developmental stage but also have the potential to become important spawning grounds for the next generation of *T. obscurus*.

Acknowledgments

The authors are grateful to the staff of Division of Urban Infrastructure Improvement, Ota City, and to the chairman Mr. Masahiro Iijima and his staff of the Tokyo Bay Recreational Fishing Boat Cooperative for granting the permission to conduct our surveys and charter boats. We thank Dr. Kana Takeyama and Mr. Kota Nakase of Penta-Ocean Construction Co., Ltd. for their useful contribution in this survey. We also thank the students of the Laboratory of Ichthyology, Tokyo University of Marine Science and Technology for their cooperation during the monthly surveys. This study was supported by JSPS KAKENHI Grant Numbers 24310028 and 15K00654 and Sasagawa Scientific Research Grant Number 2019–4094 from the Japan Science Society.

References

ANGMALISANG, D. E., K. MARUYAMA, A. HIHARA and H. KOHNO (2020): Occurrence patterns and ontogenetic intervals of *Eutaeniichthys gilli* (Gobiidae) in Obitsu-gawa river estuary, Tokyo Bay, central Japan. *La mer*, **58**, 83–99.

HERMOSILLA, J. J., Y. TAMURA, M. MOTEKI and H. KOHNO (2012): Distribution and community structure of fish in Obitsu-gawa River Estuary of inner Tokyo Bay, central Japan. *AACL Bioflux*, **5**, 197–222.

HWANG, S. Y., K. H. HAN, W. K. LEE, S. M. YOON, C. C. KIM, S. H. LEE, W. I. SEO and S. S. ROH (2006): Early life history of the *Tridentiger obscurus* (Pisces, Gobiidae). *Dev. Reprod*, **10**, 47–54.

HWANG, S. Y., J. M. PARK, S. H. LEE and K. H. HAN (2018): Osteological development of the larvae and juvenile of trident goby, *Tridentiger obscurus*. *Dev. Reprod*, **22**, 205–212.

HORINOUCHI, M. and M. SANO (2000): Food habits of fishes in a *Zostera* marina bed at Aburatsubo, central Japan. *Ichthyol. Res.*, **47**, 163–173.

HYSLOP, E. J. (1980): Stomach contents analysis: a review of method and their application. *J. Fish. Biol.*, **17**, 411–429.

KANEKO, S., K. KANOU and M. SANO (2016): Food habits of salt marsh fishes in Lake Hinuma, Ibaraki Prefecture, central Japan. *Fish. Sci.*, **82**, 631–637.

KANOU, K., T. KOIKE and H. KOHNO (2000): Ichthyofauna of tidelands in the inner Tokyo Bay, and its diversity. *Japan. J. Ichthyol.*, **47**, 115–129. (in Japanese with English abstract)

KANOU, K., H. KOHNO, P. TONGNUNUI and H. KUROKURA (2002): Larvae and juveniles of two engraulid species, *Thryssa setirostris* and *T. hamiltomi*, occurring in the surf zone at Trang, southern Thailand. *Ichthyol. Res.*, **49**, 401–405.

KANOU, K., M. SANO and H. KOHNO (2004): Food habits of fishes on unvegetated mud flat in Tokyo Bay, central Japan. *Fish. Sci.*, **70**, 978–987.

KISHI, Y. (2001): *Tridentiger obscurus*. In "*Freshwater Fishes of Japan 3rd edition*" (ed. by Kawanabe, H., N. Mizuno and K. Hosoya), Yama-Kei Publishers Co., Ltd., Tokyo, Japan, p. 605. (in Japanese)

KOHNO, H., K. KANOU and T. YOKOO (2011): A Photographic Guide to the Fishes in Tokyo Bay. Hei-

bonsya, Tokyo, Japan, 374 pp. (in Japanese)

KOHNO, H., T. YOKOO, M. MOTEKI and K. KANOU (2008): Ichthyofauna of the artificial lagoon, Shinhama-ko, located along the northernmost shore of Tokyo Bay. *Bull. Biogeogr. Soc. Japan*, **63**, 133–142. (in Japanese with English abstract)

KUWABARA, Y., N. TSUCHIDA, T. MOTOYAMA, H. KOHNO, K. KANOU, Y. SHIMADA and R. MIMORI (2003): Ichthyofauna of artificial tideland in Kasai Marine Park, Tokyo Bay. *La mer*, **41**, 28–36. (in Japanese with English abstract)

MARUYAMA, K., H. KOHNO, K. TAKEYAMA and K. NAKASE (2021): Fish assemblages and diversities in the artificial sandy beach and tidal mud flat in the inner Tokyo Bay, central Japan. *J. Tokyo Univ. Mar. Sci. Technol.*, **17**, 1–17. (in Japanese with English abstract)

MINISTRY OF THE ENVIRONMENT OF JAPAN (1997): Tidal Flats, Algal and Sea-Grass Beds and Coral Reefs in Japan. Marine parks journal, Tokyo, Japan, 291 pp. (in Japanese)

MURAI, S., A. MURASE, H. KOHNO, K. TAKEYAMA, K. NAKASE and T. IWAKAMI (2016): Fish assemblage and diversity in the developed tidal flat and sandy beach at the Furuhama Park, Ota City, Tokyo, central Japan. *La mer*, **54**, 11–27. (in Japanese with English abstract)

MURASE, A., Y. NEMOTO and H. MAEDA (2007): Gobiid fishes from Shioirino-ike, Hama-rikyu garden and Takahama canal, Tokyo Bay. *Natural History Report of Kanagawa*, **28**, 75–83. (in Japanese with English abstract)

MURASE, A., H. MAEDA and Y. NEMOTO (2013): Diet of the goby, *Tridentiger obscurus* (Teleostei: Gobiidae), inhabiting Takahama canal, the inner part of Tokyo Bay. *Bull. biogeogr. Soc. Japan*, **68**, 93–98. (in Japanese with English abstract)

NAKAIMUKI, A., D. E. ANGMALISANG, K. MARUYAMA and H. KOHNO (2022): Occurrence patterns and ontogenetic intervals based on osteological and morphometric characters of larval and juvenile gluttonous goby (*Chaenogobius gulosus*) in Furuhama Park, innermost Tokyo Bay, central Japan. *La mer*, **59**, 113–129.

NAKAMURA, N. (1942): Note on the life history of a gobioid fish, *Tridentiger obscurus* (Temminck et Schlegel). *Botany and zoology*, **10**, 115–119. (in Japanese)

OGAWA, Y (2011): A Guidebook of Gammarids in Tokyo Bay. The Faculty of Science, Toho University. http://marine1.bio.sci.toho-u.ac.jp/tokyobay/gammaridea_guide/gammaridea_tokyobay_2.0.pdf, accessed on 11 Nov. 2022. (in Japanese)

OGURA, N (1993): Tokyo Bay − Its Environmental Changes. Kouseisya-kouseikaku, Tokyo, Japan, 193 pp. (in Japanese)

OKAMURA, T., K. NAKASE, M. SATO and K. KOTERA (2004): Transition in environmental conditions of the tidal flat through its improvement and development. *Proceedings of civil engineering in the ocean*, **20**, 419–424. (in Japanese with English abstract)

ONODERA, A., K. MARUYAMA, K. TAKEYAMA and H. KOHNO (2020): Occurrence patterns of fishes collected by net cages placed at surface and bottom layers along a seawall at the Furuhama Park in innermost Tokyo Bay. *La mer*, **58**, 59–69. (in Japanese with English abstract)

OTA CITY (2015–2019): Report of the Environmental Survey at Heiwajima Canal. Division of Urban Infrastructure Development, Ota City. (in Japanese)

SAKAI, Y., M. MOTEKI and H. KOHNO (2007): Seasonal occurrence of fishes gathered with an aquatic lamp in the inner part of Tokyo Bay. *J. Tokyo Univ. Mar. Sci. Technol.*, **3**, 45–50. (in Japanese with English abstract)

SHIMIZU, M. (1990): Fishes and shellfishes in Tokyo Bay (6). *Aquabiology*, **68**, 183–189. (in Japanese with English abstract)

SHIMIZU, M. (1999): Impact of coastal development on biological environment. *Bulletin on Coastal Oceanography*, **36**, 121–130. (in Japanese)

TAKEYAMA, K., R. YAMANAKA, H. KOHNO, H. IWAMOTO, K. MIYAMOTO, R. HIRAKAWA and Y. KOZUKI (2017): Experimental study on the habitable seawall for fish in urban canal area. *Journal of JSCE, ser. B3 ocean engineering*, **73**, I_845–I_850. (in Japanese with English abstract)

TAKEYAMA, K., K. TANAKA, H. KOHNO, K. KIMURA, K.

Nakase and T. Iwakami (2018): The environmental changes of tidal flats constructed in Tokyo Bay. *Journal of JSCE, ser. B3 ocean engineering*, **74**, I_510–I_515. (in Japanese with English abstract)

Yamane, T., M. Kishida, I. Haraguchi, R. Abe, M. Daito, H. Kohno and K. Kanou (2004): Larval and juvenile ichthyofauna in artificial beaches facing Tokyo Bay. *La mer*, **42**, 35–42. (in Japanese with English abstract)

Received: January 16, 2023
Accepted: June 2, 2023

La mer 61 : 13–18, 2023, https://doi.org/10.32211/lamer.61.1-2_13
Société franco-japonaise d'Océanographie, Tokyo

Short contribution

Food habit of chiton *Acanthopleura japonica* from Jogashima, Miura peninsula, Kanagawa prefecture, Japan

Ryo MATSUMOTO[1)]* and Koetsu KON[2)]

Abstract: We examined the food habits and ontogenetic trophic shifts of the Japanese common chiton, *Acanthopleura japonica*. Specimens were collected from the intertidal zone of Jogashima, Miura Peninsula, Kanagawa Prefecture, Japan. Based on gut content analysis of 18 specimens, red algae were found to be the most abundant food item (37.0%), followed by green and brown algae (5.6% each), bivalves (5.0%), mites (2.6%), and abundant abiogenic minerals (stone or rock debris) as non-food items. This gut content composition was inconsistent with that of another population from Amakusa, Kyushu, Japan; hence, the food habits of *A. japonica* would vary depending on habitat environments, suggesting they are non-selective omnivorous feeders. Individual variations of the gut contents did not correlate with the body length, indicating *A. japonica* has no ontogenetic trophic shift. Overall, we concluded that *A. japonica* is omnivorous without an ontogenetic trophic shift.

Keywords : *Polyplacophora, diet, rocky shore, ontogeny*

1. Introduction

Chitons are a class of mollusks with eight longitudinal rows of dorsal shell plates on their backs (NISHIMURA, 1992). Most intertidal chitons are known to prey on epiphytic algae and other organisms (BARNES and HARRISON, 1994), and some authors have stated that they are herbivorous (BOOLOOTIAN, 1964; CONNOR, 1975; ROBB, 1975). However, FULTON (1975) reported that four chiton species of the genus *Mopalia* had considerable amounts of animal debris in their gut contents. LATYSHEV *et al.* (2004) found debris of coralline algae in addition to diatoms in the gut contents of *Ischnochiton hakodadensis*, *Tonicella granulate*, and *Mopalia retifera*, whereas *Lepidozona albrechti* mainly contains nematodes, shellfish, and foraminifers.

Acanthopleura japonica is the most common chiton species found on the rocky coastal intertidal shores from southern Hokkaido to Yaku Island, Japan (NISHIMURA, 1992). Although *A. ja-*

1) Graduate School of Marine Science and Technology, Tokyo University of Marine Science and Technology, 4–5–7 Konan, Minato, Tokyo 108–8477 Japan
2) Department of Ocean Sciences, Tokyo University of Marine Science and Technology, 4–5–7 Konan, Minato, Tokyo 108–8477 Japan
* Corresponding author:
E-mail: matsuryo1036@gmail.com

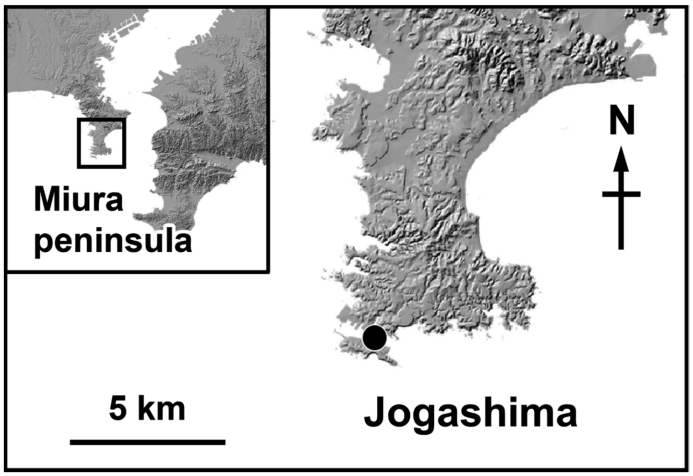

Fig. 1 Map of the intertidal rocky shore in Jogashima, Miura peninsula, Kanagawa prefecture, Japan, showing sampling station as black circle.

ponica has been widely recognized as a grazer (HUTCHINSON and WILLAMS, 2003), NISHIHAMA *et al.* (1986) reported that they mainly prey on animals such as barnacles; hence, their detailed food habits and food preferences remain unclear.

Furthermore, ontogenetic trophic shifts have not been addressed in *A. japonica*. CAMUS *et al.* (2012) reported that another *Acanthopleura* species (*A. echinata*) increased their algal diets with increase in their body size. However, this dietary shift was attributed to the variation of the niche breadth and algal richness at a local scale. The ontogenetic trophic shifts remain unclear, and this could give rise to the two different views on food habits of *A. japonica*.

Therefore, we investigated the gut contents of *A. japonica*, to evaluate the detailed food habits and the ontogenetic trophic shift.

2. Materials and methods

Sample collection

Sample collection was conducted in April 2022 at the intertidal rocky shore (35° 13.7° 'N, 139° 62.2' ° E) in Jogashima, Miura Peninsula, Kanagawa Prefecture, Central Japan (Fig. 1). The substratum in the area is composed of volcaniclastic rocks (YAMAMOTO *et al.*, 2000). We scraped *A. japonica* from the rock surface during daytime low tides using an ointment spatula, and 18 individuals were collected. Collected individuals were identified by SAITO (2017) and immediately anesthetized for several hours in a 1:1 solution of 3.2% NaCl and 7.5% MgCl following the method described by SPEISER *et al.* (2011). After anesthetization, the specimens were fixed in 70% ethanol, and their body lengths were measured with electric calipers to an accuracy of one-tenth of a millimeter.

Gut contents analysis

After body length measurements, foot muscles were cut open with postmortem scissors, and gut contents were removed and squashed on a Sedgewick-Raffer cell (1 mm × 1 mm grid slide) to a uniform depth of 1 mm. Each item was photographed with a single-lens reflex camera attached to the microscope. The area of each item was measured using ImageJ software (SCHNEID-

Table. 1 Mean percentage of specimen units consuming each food item by volume (%V, N = 18), with the ranges given within parentheses.

Category	Food item	Mean %V (Min – Max)
Minerals	Stone or rock fragments	42.0 (0.0 – 94.5)
Algae	Green algae	5.6 (0.0 – 100.0)
	Brown algae	5.6 (0.0 – 100.0)
	Red algae	37.0 (0.0 – 100.0)
Animals	Bivalves	5.0 (0.0 – 60.5)
	Mites	2.6 (0.0 – 42.2)
Others	Unknown taxa	0.3 (0.0 – 5.6)

ER *et al*., 2012) with an accuracy of 0.001 mm^2. The measured area was divided by the total area of the gut contents to calculate the percentage volume (%V) of that item (NAKANE *et al*., 2011). Food resource use was expressed as the mean percentage composition of each item by volume, which was calculated by dividing the sum of the individual volumetric percentage for the item by the number of specimens (NANJO *et al*., 2008). Items in the gut contents were identified as the lowest possible taxa based on their color and shape by SEGAWA and YAMADA (1977), NISHIMURA (1992, 1995), KUBO and MATSUKUMA (2007).

Statistical analysis

To evaluate whether *A. japonica* is carnivorous or herbivorous, the percentage volumes of animal and algal fragments were compared using the Wilcoxon signed-rank test. To evaluate the ontogenetic shift in food habits, single linear regression analyses were performed for body length as an explanatory variable and two food categories (algae and animals) as response variables. All statistical analyses were performed using R v4.2.2 (R CORE TEAM, 2022).

3. Results

A wide variety of food items were consumed by *A. japonica* (Table 1). No individual was observed with an empty gut (0.028 – 3.494 mm^2 volume, N = 18). According to the mean percentage volume of each food item, red algae were the most abundant biogenic gut content (37.0%), followed by green and brown algae (green algae, 5.6%; brown algae, 5.6%), bivalves (5.0%), and mites (2.6%). Macroalgal fragments had not been digested well and retained their color and shape. Bivalves, such as Lasaeidae retained their shape and were identified, but other shells were fragmented. The mites were not decomposed and retained their shapes. On the other hand, minerals, abiogenic stones, or rock debris, were the most abundant item (42.0%). The Wilcoxon signed-rank test revealed that the algal diet (50.4% in total) was significantly greater than the animal diet (7.3% in total) ($p < 0.01$).

The collected individuals (n = 18) showed a wide size range, with a minimum body length of 16.7 mm and a maximum of 54.3 mm. However, the body length and percentage volume of algae and animals did not show any significant regression (Fig. 2).

4. Discussion

Our study demonstrated that *A. japonica* from Jogashima, Kanagawa, central Japan, mainly fed on epiphytic algae, particularly red algal species

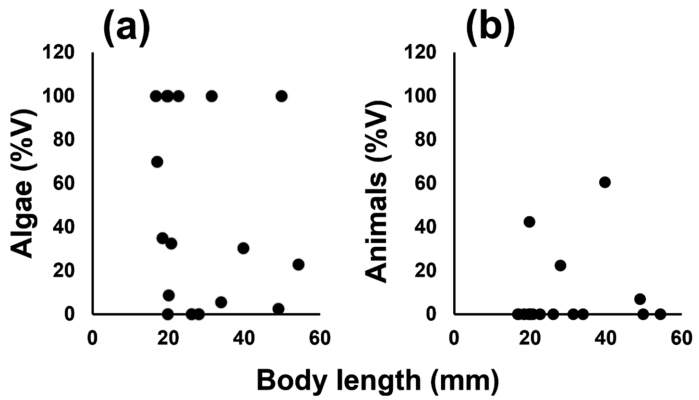

Fig. 2 Correlation diagrams between body length of *A. japonica* and minerals (a), algae (b), animals. A single linear regression analysis did not show any significant regression.

(Table 1). This result was consistent with general perceptions (HUTCHINSON and WILLAMS, 2003); however, NISHIHAMA *et al.* (1986) reported that barnacles (*Chthamalus challengeri*) were frequently found in the gut contents of *A. japonica*, in a local population of Amakusa, Kyushu, western Japan. This contradiction might be caused by the non-selective feeding of chitons. ROBB (1975) indicated that another chiton species, *Cyanoplax hartwegii*, varied its food utilization according to *in situ* food resource conditions. As a result, *A. japonica* may exhibit a variety of feeding habits depending on its habitat environment, with no specific food preferences. Another possible cause of the feeding variation could be a seasonal change in the availability of prey. The present study was conducted in April. At this time of the year, in general, macroalgae are abundant, whereas barnacles (*C. challengeri*) are present in lower density owing to the early stages of settlement (MORI, 1990). NISHIHAMA *et al.* (1986) examined the gut contents of *A. japonica* in July. At that time of the year, macroalgal biomass is typically scarce and barnacle density could have been higher owing to the late stages of settlement (MORI, 1990). Accordingly, such seasonal occurrences may have led to the feeding variation observed in *A. japonica*.

Our results also revealed that minerals such as stones and rock debris were the most abundant in the *A. japonica* gut (Table 1). Chitons, including *A. japonica*, possess robust radulae coated mainly with magnetite (LOWENSTAM, 1967) and thus feed on epiphytic organisms by scraping off the rock surface (NISHIHAMA, 1993). Such destructive feeding could have a powerful effect on removing surrounding sessile organisms (i.e., the bulldozing effect).

Body length was not correlated with either algal or animal food categories (Fig. 2), indicating that *A. japonica* has no ontogenetic trophic shift, unlike *Acanthopleura echinata* (CAMUS *et al.*, 2012). This suggests that size distribution (an ontogenetic difference) would not cause differences in food habits between the Jogashima and Amakusa populations.

Overall, the present study revealed that *A. japonica* is omnivorous without an ontogenetic trophic shift. Diet utilization can vary depending on the food environment, suggesting a non-selective feeder. Together with destructive feeding, *A. japonica* would have a substantial grazing ef-

fect on intertidal rocky shore habitats.

Acknowledgments

The authors are grateful to the anonymous reviewers for their constructive comments on the manuscript. This study was supported by JSPS KAKENHI Grant Number 22H02367.

References

Barnes, R. D. and F. W. Harrison (1994): Introduction to the Mollusca. *In* Microscopic anatomy of invertebrates. Harrison, F. W. and A. J. Kohn (eds.), Wiley-Liss, New York, p. 1–12.

Boolootian, R. A. (1964): On growth and reproduction in the chiton *Mopalia muscosa* of Santa Monica Bay. Helgoländer wiss Meeresunter-suchungen, **11**, 186–199.

Camus, A. P., A. H. Navarrete, Á. G. Sanhueza and L. F. Opazo (2012): Trophic ecology of the chiton *Acanthopleura echinata* on Chilean rocky shores. Revista Chilena de Historia Natural **85**, 123–135.

Connor, M. S. (1975): Niche apportionment among the chiton *Cyanoplax hartwegii* and *Mopalia muscosa* and the limpets *Colisella limatula* and *C. pelta* under the brown alga *Pelvetia fastigiata*. Veliger, **18**, 9–17.

Fulton, F. T. (1975): The diet of the chiton *Mopalia lignosa* (Gould, 1846). Veliger, **18**, 38–41.

Hutchinson, N. and G. A. Williams (2003): An assessment of variation in molluscan grazing pressure on Hong Kong rocky shores. Marine Biology, **142**, 495–507.

Kubo, H. and A. Matsukuma (2007): Family Lasaeidae. *In* Marine Mollusks in Japan. Okutani, T. (eds.), Tokai University press, Kanagawa, p. 1225–1227.

Latyshev, A. N., A. S. Khardin, S. P. Kasyanov and M. B. Ivanova (2004): A study on the feeding ecology of chitons using analysis of gut contents and fatty acid markers. Journal of Molluscan Studies, **70**, 225–230.

Lowenstam, H. A. (1967): Lepidocrocite, and apatite mineral, and magnetite in teeth of chitons (Polyplacophora). Science, **156**, 1373–1375.

Mori, K. (1990): Vertical variations of larval release and settlement of the intertidal barnacle, *Chthamalus challenger* Hoek. La mer, **28**, 108–187.

Nakane, Y., Y. Suda and M. Sano (2011): Food habits of fishes on an exposed sandy beach at Fukiagehama, South-West Kyushu Island, Japan. Helgoland Marine Research, **65**, 123–131.

Nanjo, K., H. Kohno and M. Sano (2008): Food habits of fishes in the mangrove estuary of Urauchi river, Iriomote island, southern Japan. Fisheries Science, **74**, 1024–1033.

Nishihama, S. (1993): Field and experimental evidence of grazing and bulldozing of a chiton on sessile invertebrate. Publications from the Amakusa Marine Biological Laboratory, Kyushu University, **12**, 37–44.

Nishihama, S., S. Nojima and T. Kikuchi (1986): Distribution, diet and activity of a chiton *Liolophura japonica* (Lischke), in Amakusa, west Kyushu. Publications from the Amakusa Marine Biological Laboratory, Kyushu University, **8**, 113–123.

Nishimura, S. (1992): Guide to seashore animals of Japan with color pictures and keys, **I**. Hoikushya, Osaka, 425 pp.

Nishimura, S. (1995): Guide to seashore animals of Japan with color pictures and keys, **II**. Hoikushya, Osaka, 663 pp.

R core team. (2022): A language and environment for statistical computing. R Foundation for Statistical Computing, Vienna, Austria.

Robb, M. F. (1975): The diet of the chiton *Cyanoplax hartwegii* in three intertidal habitats. Veliger, **18**, 34–37.

Saito, H. (2017): Familiy Chitonidae. *In* Marine Mollusks in Japan. Okutani, T. (eds.), Tokai University press, Kanagawa, p. 733–735.

Schneider, C. A., W. S. Rasband and K. W. Eliceiri (2012): NIH image to IMAGEJ, 25 years of image analysis. Nature Methods, **9**, 671–675.

Segawa, S. and Y. Yamada (1977): Coloured illustrations of the seaweeds of Japan. Hoikusha, Osaka, 195 pp.

Speiser, I. D., D. J. Eernisse and S. Johnsen (2011): A chiton uses aragonite lenses to form images.

Current Biology, **21**, 665–670.

YAMAMOTO, Y., Y. OHTA and Y. OGAWA (2000): Implication for the two-stage layer-parallel faults in the context of the Izu forearc collision zone: examples from the Miura accretionary prism, Central Japan. Tectonophysics, **325**, 133–144.

Received: January 25, 2023
Accepted: May 4, 2023

La mer 61 : 19–29, 2023, https://doi.org/10.32211/lamer.61.1-2_19
Société franco-japonaise d'Océanographie, Tokyo

Characteristics of the two types of Kuroshio large meanders

Hiroyuki YORITAKA[1)]*, Atsushi KUBOKAWA[2)] and Kimio HANAWA[3)]

Abstract: There are two types of Kuroshio large meanders: the large meander west (LMW), whose trough (the southernmost point) is located west of the Izu-Ogasawara Ridge, and the large meander east (LME), whose trough is located on the ridge. We compared the characteristics of LMW and LME using accumulated Kuroshio path data. Comparing the five LMWs and three LMEs, the central latitude of the meanders of the LME was higher than that of the LMW, and the amplitude of the meanders of the LME was smaller than that of the LMW. Fitting the solution of the path equation to the Kuroshio path, the initial path direction of the LME was smaller than that of the LMW, but the characteristic velocities and meander wavelengths of the LME were not significantly different from those of the LMW. The difference in longitude between the LME and LMW troughs is due to the difference in separation longitude, not the difference in meander wavelength associated with the difference in characteristic velocity.

Keywords : *Kuroshio, large meander, Rossby lee wave, path equation*

1. Introduction

The Kuroshio in the Shikoku Basin exhibits two modes, namely, a straight path (blue line in Fig. 1) and a large meander path (red line in Fig. 1), as described in STOMMEL and YOSHIDA (1972). Both paths enter the Pacific Ocean from approximately 130° E and 30° N, Tokara Strait south of Kyushu, and pass north of Hachijojima (33° N) on the Izu-Ogasawara Ridge, which extends north-south at approximately 140° E. From the dynamic perspective, ROBINSON and TAFT (1972), using the path equation (ROBINSON and NILLER, 1967), regarded the large meander path as a Rossby lee wave that separated from the continental slope off the south coast of Shikoku (132° E-135° E). WHITE and MCCREARY (1976) regarded the large meander path as a Rossby lee wave generated by bypassing Kyushu. They considered that, since the wavelength of a linear Rossby wave is proportional to the square root of the current velocity, a large meander path exists if the current velocity of the Kuroshio is in the range where the entire large meander path (one and half wavelengths) is shorter than the distance between Kyushu and the Izu-Ogasawara Ridge; the large meander path does not appear if the current velocity is higher than that range.

MASUDA (1982), using the path equation, showed that, within a specific current velocity range, multiple equilibria can exist for which

1) Kuroshio Science Unit, Kochi University, Monobe-Otsu 200, Nankoku, Kochi, 783–8502, Japan
2) Faculty of Environmental Earth Science, Hokkaido University, N10W5, Sapporo, Hokkaido, 060–0810, Japan
3) Yamagata University, Kojirakawa 1–4–12, Yamagata, Yamagata, 990–8560, Japan

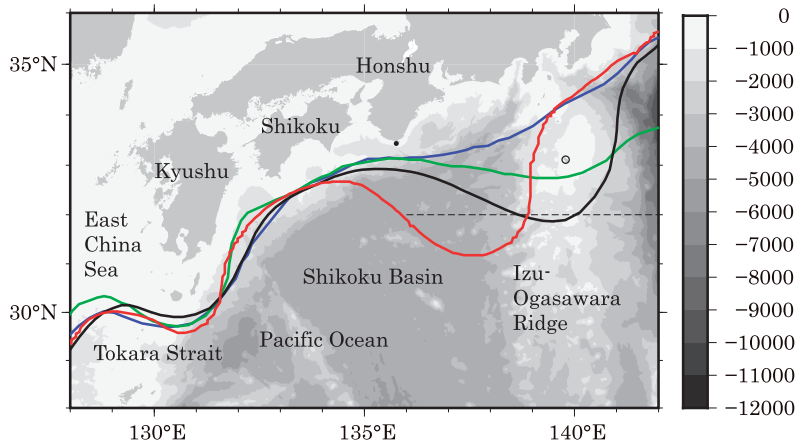

Fig. 1 Map around the Shikoku Basin and the typical path (solid line) for four modes of the Kuroshio path based on the QBOC (Quick Bulletin of Ocean Conditions); the non-large meander north (NLMN: blue), non-large meander south (NLMS: green), large meander east (LME: black), and large meander west (LMW: red). Dashed line indicates 32° N line. Open circle indicates Hachijojima, closed circle indicates Cape Shionomisaki. Color scale is for water depth. ETOPO1 was used for bathymetric data.

there are both straight and large meander paths through the inlet, that is Tokara Strait and outlet of the Izu-Ogasawara Ridge at different latitudes. Subsequently, several regional models driven by inflow and outflow with different latitudes obtained multiple equilibrium solutions in specific velocity ranges (Chao, 1984; Yasuda *et al.*, 1985; Yoon and Yasuda, 1987; Akitomo *et al.*, 1991).

Tsujino *et al.* (2006) and Tsujino *et al.* (2013) drove the ocean general circulation model with historical winds and reproduced the Kuroshio large meander, although it did not necessarily match the actual period of occurrence. Tsujino *et al.* (2013) noted that the meander tended to decay as the Kuroshio transport increased. Usui *et al.* (2013) also showed that Sverdrup transport in the Shikoku Basin increased at the last stage of the historical Kuroshio large meander.

Yoshida *et al.* (2014) statistically analyzed the Kuroshio path in the Quick Bulletin of Ocean Conditions (QBOC) issued by the Japan Coast Guard, and proposed another large meander path (large meander east: LME) whose trough (southernmost point) is located south of 32° N, similar to the conventional large meander path (large meander west: LMW), but with a much different longitude. While the trough of the LMW is located west of the Izu-Ogasawara Ridge, the trough of the LME is located on the ridge. Figure 1 shows typical paths for the four modes of the Kuroshio path classified by Yoshida *et al.* in the QBOC. If the southernmost latitude of 136° E-142° E is north of 32° N, the path is a non-large meander; else, if the southernmost latitude of 136° E-142° E is south of 32° N, the path is a large meander. The non-large meander path passing north of Hachijojima (see Fig. 1) is the non-large meander north (NLMN); the non-large meander path passing south of Hachijojima is the non-large meander south (NLMS); the large meander path passing north of Hachijojima

is the LMW, and the large meander path passing south of Hachijojima is the LME. YOSHIDA *et al.* classified the Kuroshio paths from 1970 to 2009 and showed that the LMW accounted for 23 % in terms of time and the LME accounted for 9 %.

The purpose of this study is to elucidate the differences in the characteristics of the LMW and LME. In particular, we will estimate the characteristic velocities of the LMW and LME by the path equation and investigate whether the velocity of the Kuroshio controls the appearance and disappearance of the LMW, as suggested by WHITE and MCCREARY.

2. Data and method

2.1 Kuroshio path

As the Kuroshio path, the current axis of the Kuroshio path drawn in the QBOC (Quick Bulletin of Ocean Conditions) was used. In the QBOC, the Kuroshio path fixed at a width of 40 nautical miles (approximately 74 km) is drawn based on the analysis of the observed data of current, sea surface temperature, and 200-m-depth temperature. The QBOC has been issued twice a month since April 1960, once a week since April 2001, and daily on weekdays since August 2006. We used the line data created by the Japan Hydrographic Association from the QBOC image data (JAPAN HYDROGRAPHIC ASSOCIATION, 2022). The current axis was defined as the location of 13 nautical miles (approximately 24 km) from the coastal side of the Kuroshio path. In addition, since August 2006, we used only the data issued on Wednesdays, as in the case of the earlier data.

For all modes in Fig. 1, the Kuroshio seems to flow along the coast after entering the Pacific Ocean at 130° E-131° E. For the NLMN, the Kuroshio flows along the coast to near Cape Shionomisaki (135.76° E). For the NLMS, the path has a crest (northernmost point) near Cape Shionomisaki and flows southward at a small angle to the latitude line, and it turns northward with a trough at 139° E-140° E. For the LME, the path leaves the coast at 135° E-136° E as a crest and flows southward, and it turns northward with a trough at 139° E-140° E. For the LMW, the path leaves the coast and flows southward with a crest at 134° E-135° E, and it turns northward with a trough at 137° E-138° E. For both large meander paths, the LME and LMW, the path between the crest and trough has the form of a sine wave, and it is presumed to be a free Rossby lee wave.

Figure 2 shows the mode of the Kuroshio path in the QBOC from 1972 to 2019. There were eight large meander periods of LME or LMW that lasted more than one year (thick solid line in Fig. 2). The 8th large meander period, which began in 2017, continues through 2020 and beyond. Figure 3 shows the Kuroshio paths for each large meander period, and Table 1 shows the appearance frequency of each path mode during each large meander period. LME is dominant in 1999–2001 and 2008–2009; LME and LMW are comparable in 1981–1984 and 1989–1991.

2.2 Path equation and its property

The path equation derived by ROBINSON and NIILER (1967) was used. Assuming that the current velocity at the sea bottom is zero, the path equation can be written as follows:

$$U\left(\frac{d\theta}{dy}-\kappa_0\right)+\beta(Y-Y_0)=0 \qquad (1)$$

where U is the characteristic velocity $\left(\frac{\langle v^2\rangle}{\langle v\rangle}\right)$ (v is the current velocity in the path direction), and $\langle\ \rangle$ denotes the surface integral over the cross-section of the path. θ is the path direction from east, y is the coordinate of the path direction, $\left|\frac{d\theta}{dy}\right|$ is the curvature of the path,

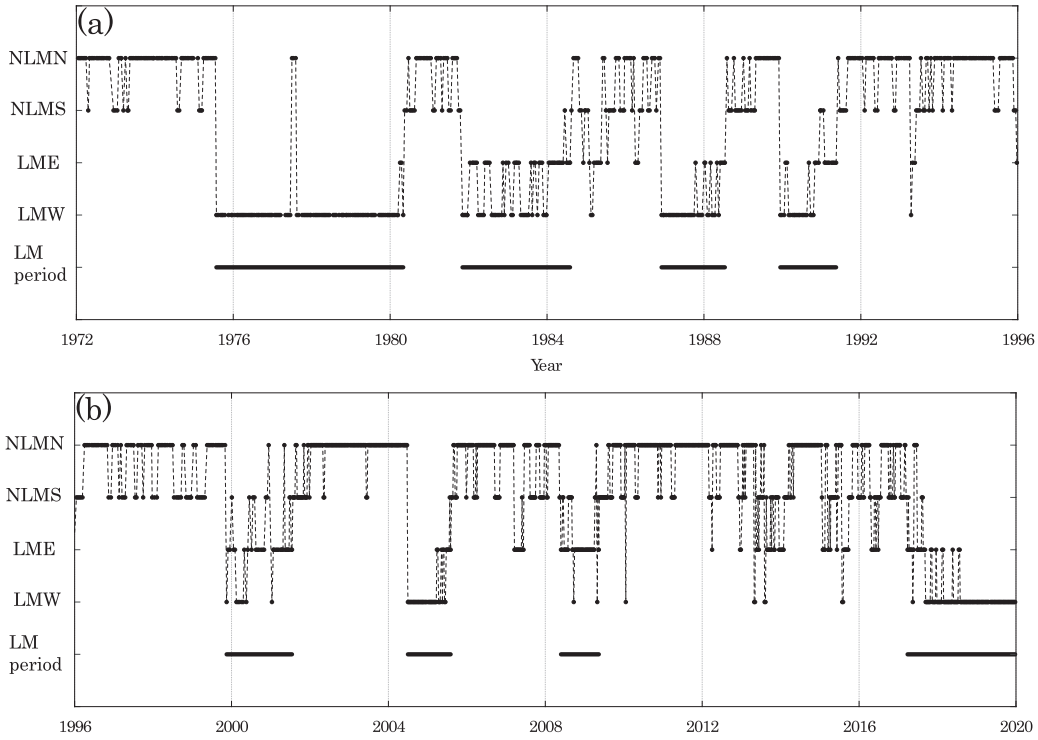

Fig. 2 Mode of the Kuroshio path (small closed circle and dashed line). (a) 1972–1995, (b) 1996–2019. Thick solid line indicates large meander periods of more than one year.

and κ_0 is $\left(\frac{d\theta}{dy}\right)$ at the initial position of the path (X_0, Y_0) (the parameters are shown in Fig. 4). β is the meridional variation $\left(\frac{df}{dY}\right)$ of the Coriolis parameter f. Equation (1) represents the conservation of the potential vorticity of a thin jet, with the first term on the left side representing the relative vorticity, and the second term on the left side representing the planetary vorticity. The characteristic velocity coincides with the current velocity if the current is spatially uniform, and when the velocity has a jet-like profile, it is positively correlated with the maximum velocity, but it is much lower than the maximum velocity. Robinson and Taft (1972) varied the characteristic velocity of the Kuroshio in the Shikoku Basin in the range of 0.2–1.0 m/s and tried to change the path. Assuming that the initial curvature is zero, the path is determined by the initial path direction θ_0 and the characteristic velocity U. Figure 5 shows the variation in the path due to the variation in the initial path direction θ_0 and the characteristic velocity U. If the initial path direction is in this range, the form of the path is close to a sine wave, and the larger the initial path direction, the larger the amplitude and the shorter the wavelength. On the other hand, the higher the characteristic velocity, the larger the amplitude and the longer the wavelength is.

A steady jet with a north-south component follows the path equation if there is no generation or dissipation of vorticity owing to contact with the lateral or bottom boundary. Then, the jet

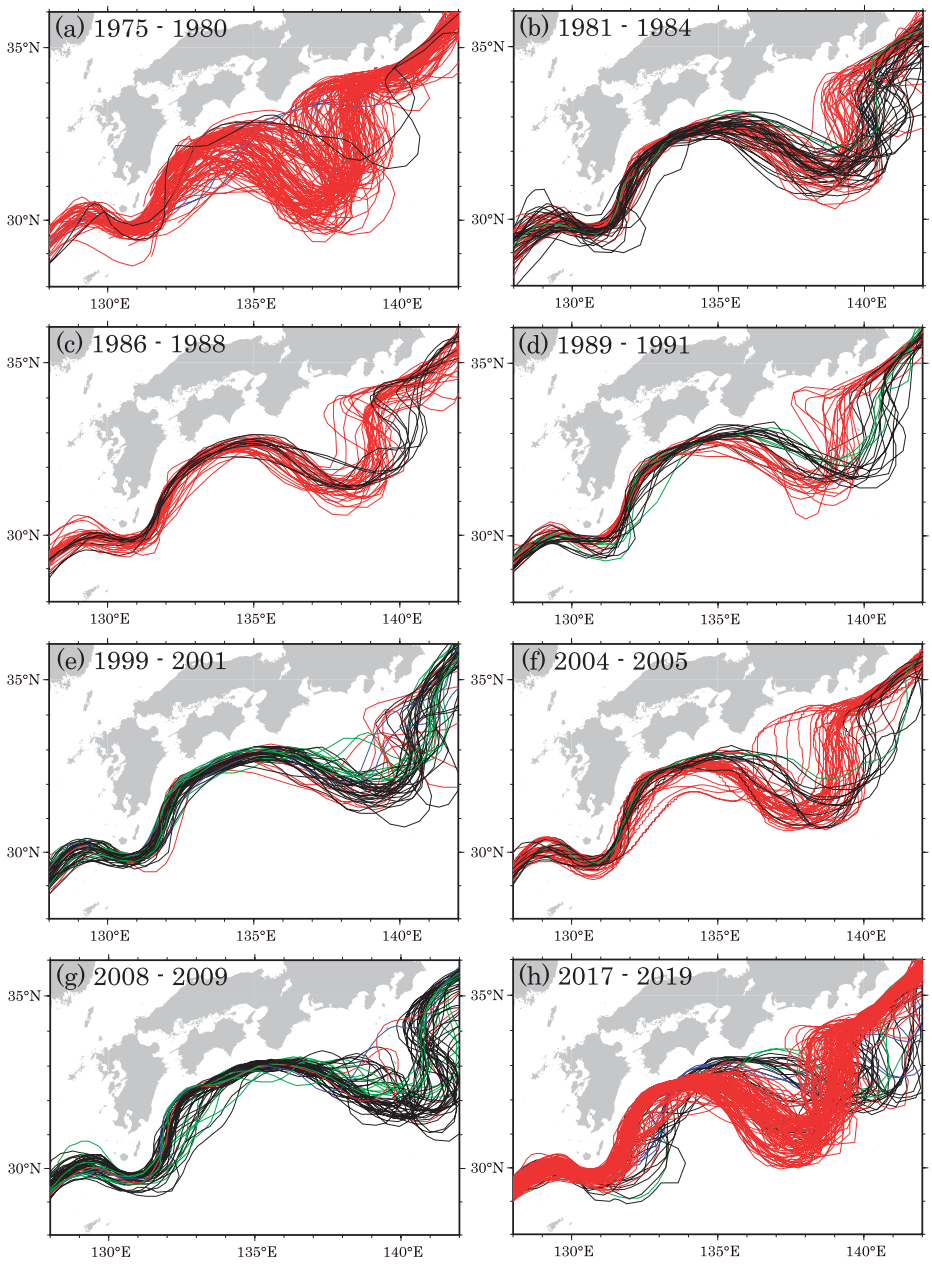

Fig. 3 Kuroshio path based on the QBOC. NLMN (blue), NLMS (green), LME (black), and LMW (red).

heads east while meandering as a Rossby lee wave. This equation does not allow us to discuss the path near the lateral boundary or in shallow waters, and therefore, we cannot definitely state how the western boundary current separates from the lateral boundary. However, considering that the western boundary current flowing from the south along the boundary separates

Table. 1 Appearance frequency of each path mode during each large meander period.

No	Period	Frequency of each path mode			
		NLMN	NLMS	LME	LMW
1	1975 Jul. - 1980 May	3	0	2	102
2	1981 Nov. - 1984 Aug.	0	1	35	30
3	1986 Dec. - 1988 Jul.	0	0	9	31
4	1989 Dec. - 1991 May	0	3	14	18
5	1999 Nov. - 2001 Jul.	2	8	30	8
6	2004 Jun. - 2005 Aug.	0	1	11	44
7	2008 May - 2009 May	1	10	37	2
8	2017 Mar. - 2019 Dec.	4	3	24	112

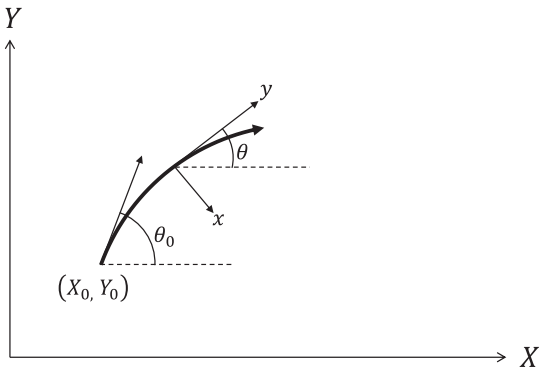

Fig. 4 Parameters in the path equation.

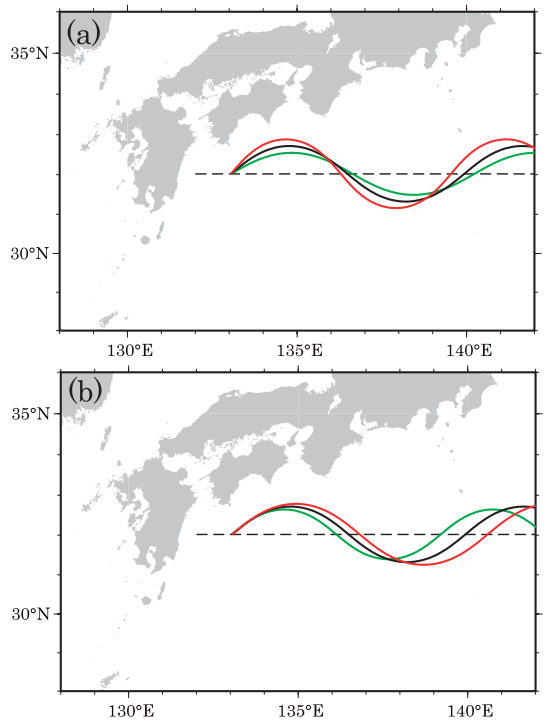

Fig. 5 Variation in the solution of the path equation due to changes in (a) the initial path direction 30° (green), 40° (black) and 50° (red) for the characteristic velocity 0.25 m/s, and (b) the characteristic velocity 0.20 m/s (green), 0.25 m/s (black) and 0.30 m/s (red) for the initial path direction 40°.

from the boundary as the relative vorticity decreases due to the β effect, as shown in Fig. 6, the latitude of separation point is Y_0 where the path has zero curvature, and the boundary direction becomes the initial path direction θ_0. The separation point is the point where vorticity is supplied by contact with the boundary immediately upstream and potential vorticity is conserved downstream of it.

3. Characteristics of large meanders

Figure 7 shows the ten mean paths for the eight large meander periods shown in Table 1, along with their standard deviations at the crests and troughs; for 1981–1984 and 1989–1991, the mean paths of both the LMW and LME were determined. The mean path was determined as the mean latitude of the path for every 0.05 degrees of longitude from 128° E to just east of the trough. The mean was taken by excluding the paths farthest from the mean path until all paths were within 0.8 degrees of latitude from the mean path. The horizontal broken lines in Fig. 7 are the central latitudes of the crest and trough of each mean path. In our model shown in Fig. 6, the central latitude coincides with the latitude of the separation point, because the curvature of the path is zero there. The 2000 m isobath east of Kyushu and south of Shikoku extends approximately 60 degrees (from the east) south of 31.5° N and approximately 30 degrees (from the east)

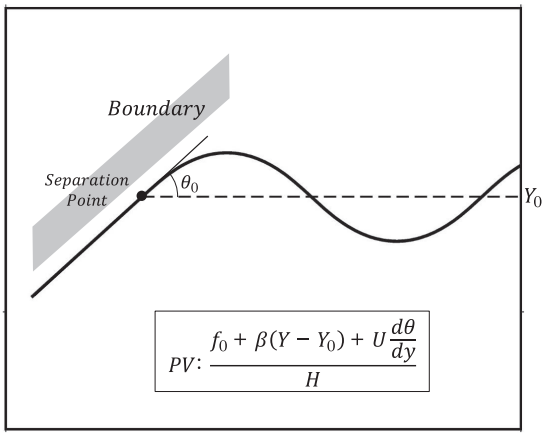

Fig. 6 Schematic diagram of the separation of the western boundary current and the Rossby lee wave. PV denotes the potential vorticity of the thin jet separated from the coast, f_0 denotes the Coriolis parameter at Y_0, β denotes the meridional variation of the Coriolis parameter, U denotes the characteristic velocity, and H denotes the height of the water column, which is constant along geostrophic streamlines in the one-layer reduced gravity model. $Ud\theta/dy$ is the relative vorticity. The parameters are shown in Fig. 4.

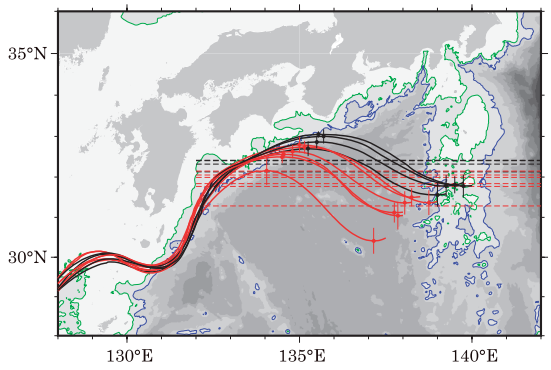

Fig. 7 Mean path (solid line) and central latitude (dashed line) of the Kuroshio path. The circles indicate the crests and troughs, and the thin vertical lines indicate standard deviations at the crests and troughs. LME (black), and LMW (red). The green line indicates the 1000 m isobath and the blue line indicates the 2000 m isobath. Color scale of water depth is same as in Fig. 1.

north of 31.5° N. The mean path of the large meander, except for 1975–1980 (LMW), seems to lie on the 2000 m isobath south of 31.5° N, and on the 1000 m isobath south of Shikoku. The separation point is the intersection of the central latitude and the mean path. The five LMW separation points, except 1975–1980, are on the transition from the 2000 m isobath to the 1000 m isobath, and the three LME separation points, except 1981–1984, are on the 1000 m isobath south of Shikoku.

Figure 8 shows the optimal solution of the path equation fitted to the path between the crest and trough for each mean path (Fig. 7). The solution of the path equation has zero curvature at the central latitudes of the crest and trough of the mean path. By varying the initial path direction θ_0 in steps of 1 degree, the characteristic velocity U in steps of 0.01 m/s, the combination of initial path direction and characteristic velocity that minimizes the root-mean-square difference in latitude between the mean path and the solution between the crest and trough in the mean path was determined. Figure 8 shows that the solution of the path equation does not fit the mean path in the west of the crest except 1975–1980 period. The paths seem to lie on the 1000 m isobath south of Shikoku, which elongates the length between the separation point and the crest. Although the details are unclear, it seems that the continental slope strongly affects the path through a mechanism not considered in the thin jet theory.

Table 2 shows the parameters of the optimal solution. As typical values of LMW, we use the mean of the five LMW except for 1975–1980, and as typical values of LME, we use the mean of the three LME except for 1981–1984. Table 2 shows the mean and standard deviation for LMW and

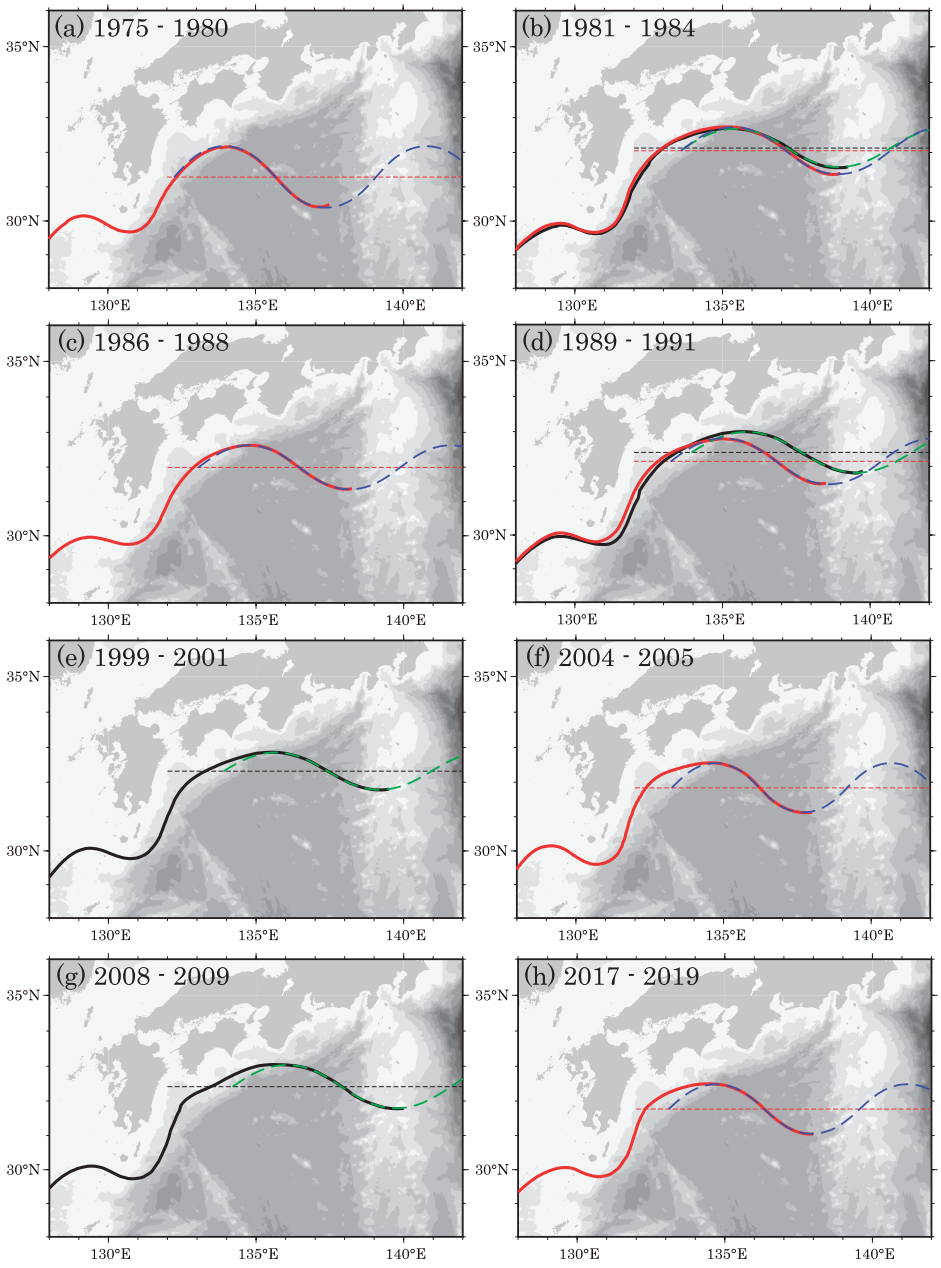

Fig. 8 Optimal solution (dashed line) of the path equation fitted to the mean path of the Kuroshio (solid line). Thin dashed line indicates the central latitude. Black and green lines indicate LME; red and blue lines indicate LMW. Color scale of water depth is same as in Fig. 1.

Table. 2 Parameters of optimal solution.

Period	Mode	Central latitude [degrees]	Amplitude [degrees]	Initial path direction [degrees]	Characteristic velocity [m/s]	Trough longitude [degrees]	Seperation longitude [degrees]	3/4Wave-length [degrees]	Elongation [degrees]
1975 - 1980	LMW	31.29	0.89	49	0.28	137.37	132.32	5.12	-0.07
1981 - 1984	LMW	32.05	0.68	38	0.26	138.92	132.84	5.32	0.76
1986 - 1988	LMW	31.99	0.64	37	0.24	138.18	132.88	5.13	0.17
1989 - 1991	LMW	32.15	0.66	37	0.26	138.60	132.82	5.35	0.43
2004 - 2005	LMW	31.84	0.71	46	0.20	137.70	132.37	4.45	0.88
2017 - 2019	LMW	31.77	0.72	43	0.23	137.95	132.30	4.85	0.80
Mean for LMW		**31.96**	**0.68**	**40**	**0.24**	**138.27**	**132.64**	**5.02**	**0.61**
Standard deviation		**0.15**	**0.03**	**4**	**0.02**	**0.49**	**0.28**	**0.38**	**0.30**
1981 - 1984	LME	32.13	0.55	32	0.24	138.94	133.00	5.24	0.70
1989 - 1991	LME	32.40	0.59	32	0.27	139.54	133.45	5.59	0.50
1999 - 2001	LME	32.32	0.54	31	0.24	139.18	133.28	5.28	0.62
2008 - 2009	LME	32.41	0.62	34	0.27	139.74	133.47	5.54	0.73
Mean for LME		**32.38**	**0.58**	**32**	**0.26**	**139.49**	**133.40**	**5.47**	**0.62**
Standard deviation		**0.05**	**0.04**	**2**	**0.02**	**0.28**	**0.10**	**0.17**	**0.12**

LME, respectively, and three of the eight parameters, characteristic velocity, wavelength, and elongation, are not significantly different between LMW and LME ($0.05 <$ p: probability value). The mean central latitude of the LME is 0.42 degrees higher than that of the LMW. The mean amplitude of the north-south meander of the LME is 0.10 degrees smaller than that of the LMW. The mean initial path direction of the LME is 8 degrees smaller than that of the LMW, which makes the amplitude smaller.

Figure 9 shows the latitudinal distribution of the direction (from the east) of the mean path east of Kyushu and south of Shikoku obtained by central difference ($\theta_i = \tan^{-1}\left(\frac{Y_{i+1} - Y_{i-1}}{2\Delta X}\right)$), as well as the initial path direction of the optimal solution at the central latitude. Both the mean path direction and the initial path direction decrease with latitude. In the central latitude range, 31.77° N to 32.41° N, except for 1975–1980, the decrease in initial path direction with increasing latitude is less than that in the mean path direction. The initial path direction depends on the central latitude, but differs slightly from the mean path direction, possibly due to the effect of the continental slope as well as elongation.

Whether the Kuroshio passes north or south of Hachijojima depends on the longitude of the trough, which divides the LMW and LME (see Fig. 7). The longitude of the trough is the sum of the longitude of the separation point, the elongation south of Shikoku and three-quarters of the wavelength. The mean longitude of the LME trough is 1.22 degrees larger than the mean longitude of the LMW trough (Table 2). Since there is no significant difference in wavelength and elongation between LME and LMW, the difference in longitude of the trough is generated by the 0.76 degrees' difference in longitude of the separation point. Although the wavelength depends on the characteristic velocity and the initial path direction, there is no sig-

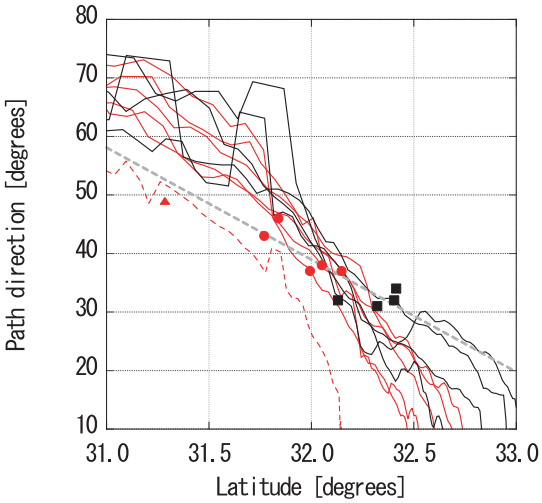

Fig. 9 Direction of the mean path at each latitude (lines) and the initial path direction of the optimal solution at the central latitude (marks). LMW (red) and LME (black). The dashed red line and triangle indicate 1975–1980 LMW. The gray dashed straight line represents the regression line for the nine marks except for the 1975–1980 LMW.

nificant difference in wavelength between LME and LMW because there is no significant difference in characteristic velocity and the dependence on the initial path direction is weak.

On the other hand, the longitude of the LMW trough for the 1975–1980 is 0.90 degrees less than the LMW mean. The large factors are the difference in elongation of 0.68 degrees and the difference in longitude of the separation point of 0.32 degrees. Elongation for the 1975–1980 period, when the path does not reach the 1000 m isobath south of Shikoku, is almost zero.

The 1981–1984 LME and LMW trough longitudes are nearly equal, almost in the middle of the LME mean and the LMW mean. This suggests that the trough of the 1981–1984 large meander alternated between LME and LMW paths because it was located near the boundary longitude where the LME and LMW are divided.

4. Discussion

The initial path direction and characteristic velocity were estimated by fitting solutions of the path equation to two types of Kuroshio large meanders, LMW and LME paths. A comparison of the five LMWs and three LMEs showed no significant differences in characteristic velocities and, therefore, no significant differences in meander wavelengths. The difference in the longitude of the meander troughs was due to the difference in the longitude at which the Kuroshio separates from the continental slope east of Kyushu or south of Shikoku. This differs from the estimation by White and McCreary (1976), who suggested that the troughs shift over the Izu-Ogasawara Ridge due to the increased velocity of the Kuroshio and the longer wavelengths of the Rossby lee waves.

As pointed out by Yoshida *et al.* (2014), at the last stage of the LMW-dominated large meander period, the Kuroshio path becomes the LME and transitions to the NLMS (non-large meander south), ending the large meander. This transition of the Kuroshio path can be seen as a northward shift of the separation latitude from the continental slope. The increase in Kuroshio volume transport at the last stage of the large meander period found by Tsujino *et al.* (2013) and Usui *et al.* (2013) may cause a northward shift in the separation latitude without an increase in characteristic velocities.

The path of the Kuroshio large meander deviates from the optimal solution of the path equation once it passes the trough, and flows northward over the western slope of the Izu-Ogasawara Ridge for LMW and over the eastern slope of the ridge for LME, mostly along the isobathic line. However, depths at the deviation points ranged from 4000 m and deeper in 1975–

1980 to approximately 1000 m near the top of the Izu-Ogasawara Ridge in some LMEs. This suggests that the deviation from the solution near the Izu-Ogasawara Ridge is not due to the local effect of the bottom topography.

Acknowledgments

We thank two reviewers for their helpful comments. For the Kuroshio path, we used the data digitized by the Japan Hydrographic Association of the QBOC issued by the Japan Coast Guard (JAPAN HYDROGRAPHIC ASSOCIATION, 2022). We used the bathymetric data ETOPO1 (AMANTE and EAKINS, 2009) provided by National Oceanic and Atmospheric Administration. We thank these institutions for their data. The Generic Mapping Tools version 6 (WESSEL *et al.*, 2019) was used to draw maps.

References

AMANTE, C. and B. W. EAKINS (2009): ETOPO1 1 arc-minute global relief model: procedures, data sources and analysis. NOAA Technical Memorandum NESDIS NGDC-24. Boulder, CO: National Geophysical Data Center.

AKITOMO, K., T. AWAJI and N. IMASATO (1991): Kuroshio path variation south of Japan: 1. Barotropic inflow-outflow model. Journal of Geophysical Research, **96** (C2), 2549–2560.

CHAO, S. -Y. (1984): Bimodality of the Kuroshio. Journal of Physical Oceanography, **14** (1), 92–103.

JAPAN HYDROGRAPHIC ASSOCIATION (2022): Kuroshio Current Path Dataset 2021 Ed. (1955–2021).

MASUDA, A. (1982): An interpretation of the bimodal character of the stable Kuroshio path. Deep Sea Research Part A. Oceanographic Research Papers, 29 (4), 471–484.

ROBINSON, A. R. and P. P. NIILER (1967): The theory of free inertial currents I. Path and structure. Tellus, **19** (2), 269–291.

ROBINSON, A. R. and B. A. TAFT (1972): A numerical experiment for the path of the Kuroshio. Journal of Marine Research, **30**, 65–101.

STOMMEL, H. and K. YOSHIDA (1972): Kuroshio; its physical aspects. Tokyo, University of Tokyo Press.

TSUJINO, H., S. NISHIKAWA, K. SAKAMOTO, N. USUI, H. NAKANO and G. YAMANAKA (2013): Effects of large-scale wind on the Kuroshio path south of Japan in a 60-year historical OGCM simulation. Climate Dynamics, **41**, 2287–2318.

TSUJINO, H., N. USUI and H. NAKANO (2006): Dynamics of Kuroshio path variations in a high-resolution GCM. Journal of Geophysical Research, **111** (C11), C11001.

USUI, N., H. TSUJINO, H. NAKANO and S. MATSUMOTO (2013): Long-term variability of the Kuroshio path south of Japan. Journal of Oceanography, **69**, 647–670.

WESSEL, P., J. F. LUIS, L. UIEDA, R. SCHARROO, F. WOBBE, W. H. F. SMITH and D. TIAN (2019): The Generic Mapping Tools version 6. Geochemistry, Geophysics, Geosystems, **20** (11), 5556–5564.

WHITE, W. B. and J. P. MCCREARY (1976): On the formation of the Kuroshio meander and its relationship to the large-scale ocean circulation. Deep Sea Research and Oceanographic Abstracts, **23** (1), 33–47.

YASUDA, I., J.-H. YOON and N. SUGINOHARA (1985): Dynamics of the Kuroshio large meander-barotropic model. Journal of the Oceanographical Society of Japan, **41**, 259–273.

YOON, J.-H. and I. YASUDA (1987): Dynamics of the Kuroshio large meander: two-layer model. Journal of Physical Oceanography, **17** (1), 66–81.

YOSHIDA, J., E. MAETA, N. NAKANO, H. DEGUCHI and M. NEMOTO (2014): Statistical analysis of the variation of the Kuroshio path, Oceanography in Japan, **23**, 171–196 (in Japanese with English abstract and legends)

Received: July 12, 2023
Accepted: October 26, 2023